

Molecular Encapsulation beyond the Aperture Size Limit through Dissociative Linker Exchange in Metal–Organic Framework Crystals

Joseph V. Morabito,[†] Lien-Yang Chou,[†] Zhehui Li, Cesar M. Manna, Christopher A. Petroff, Rutvin J. Kyada, Joseph M. Palomba, Jeffery A. Byers,* and Chia-Kuang Tsung*

Department of Chemistry, Merkert Chemistry Center, Boston College, Chestnut Hill, Massachusetts 02467, United States

S Supporting Information

ABSTRACT: Under linker exchange conditions, large guests with molecular diameters 3–4 times the framework aperture size have been encapsulated into preformed nanocrystals of the metal–organic framework ZIF-8. Guest encapsulation is facilitated by the formation of short-lived “open” states of the pores upon linker dissociation. Kinetic studies suggested that linker exchange reactions in ZIF-8 proceed via a competition between dissociative and associative exchange mechanisms, and guest encapsulation was enhanced under conditions where the dissociative pathway predominates.

Incorporating functional guest molecules into the cavities of crystalline porous materials makes it possible to engineer these materials for drug delivery,^{1a,b} sensing,^{1c,d} electrical conductivity,^{1e,f} luminescence,^{1g–i} and energy conversion.^{1j–l} Host–guest crystalline porous materials have been studied in aluminosilicate zeolites since the 1980s.² Recently, attention has been drawn to a molecular-type class of crystalline porous materials, metal–organic frameworks (MOFs), which offer more opportunities for host–guest composites compared with zeolites because of their chemically tunable pore surfaces, comparatively mild syntheses, and unique properties such as framework flexibility,^{3a} post-synthetic modification,^{3b} and exchangeable ligands.^{3c,d} The great diversity of MOF properties and structure types has led to various approaches for the synthesis of host–guest composites.^{3b,4}

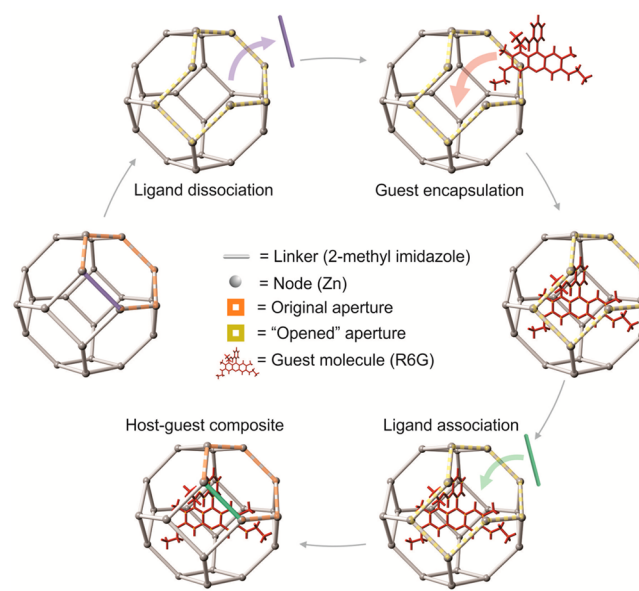
Despite these advances, approaches for incorporating large and more diverse guests are still limited to a few specific MOF types. For example, negatively charged MOFs have been utilized to incorporate cationic organic compounds and metals,⁴ and MOFs with unoccupied sites can encapsulate guests through dative bonds.^{1e} Despite these successes, many MOFs lack framework charge or unoccupied sites, prohibiting the general applicability of these methods. Alternatively, guest molecules have been covalently bound to the bridging ligands of the frameworks,^{3b} but the loss of degrees of freedom for tethered homogeneous catalysts could lead to decreased activity or selectivity in catalytic applications.⁵

The incorporation of guest molecules into MOFs by diffusion is generally limited to guests that are smaller than the MOF aperture size.^{4b} This limitation commonly leads to guest molecule leaching, which is particularly problematic for catalytic applications. Retaining guests in the cavities of MOFs by pursuing strategies that incorporate guests larger than the MOF

aperture size could circumvent this problem. Two strategies for this are ship-in-a-bottle assembly of the guest within the pore subunits and de novo encapsulation of the guest during MOF crystal growth.^{4a,6} The ship-in-a-bottle approach is challenging for the assembly of guest molecules that require multiple postsynthetic operations. The de novo encapsulation approach does not have this limitation, but it requires that guest molecules not perturb MOF crystal growth and be compatible with the conditions used for MOF synthesis.

Herein we introduce a new concept for incorporating larger and more diverse guest molecules into MOFs (Scheme 1). In this approach, we take advantage of ligand exchange reactions to “open” part of the framework of the presynthesized MOF crystals. Expanded apertures created by the ligand exchange process allow large guest molecules to diffuse into the MOF pores. After guest incorporation, association of the ligands closes the large apertures, trapping the guest molecules in the MOF pores. This new approach to guest incorporation is expected to be general because framework ligand exchange has been carried out under various conditions and exists in a large number of MOFs with diverse secondary building units.^{3c,d,7–14} An

Scheme 1



Received: May 31, 2014

Published: August 21, 2014

additional practical advantage of decoupling encapsulation and MOF synthesis is that MOF production can be scaled-up independently of guest loading, which is especially relevant since several MOFs, such as ZIF-8, Fe-BTC, HKUST-1, and MIL-53(Al), have become commercially available.

It has been reported that the bridging organic ligands in MOF crystals can be exchanged with compatible but chemically distinct ligands without disrupting the underlying MOF crystal structure and morphology. This phenomenon was first reported by Choe for pillared porphyrin paddlewheel frameworks¹² and has been optimized by several groups.^{8,9} The ligand exchange process has become extremely popular for the diversification of MOFs and is most commonly called solvent-assisted linker exchange (SALE)⁸ or postsynthetic exchange (PSE).⁹ In order to avoid confusion between MOF bridging ligands and guest molecules that may serve as ligands for transition-metal guests, we henceforth will refer to framework bridging ligands as “linkers”.

The ability of ligands to be exchanged between metal centers is ubiquitous in coordination chemistry, where the two limiting pathways for ligand substitution reactions are associative or dissociative mechanisms. In a MOF, the metal centers are typically coordinatively saturated, a property that we reasoned would make a dissociative mechanism more likely. If dissociative linker substitution occurs in MOFs, we hypothesized the existence of short-lived linker vacancies that would momentarily expand the pore aperture size to allow the passage of larger guests into the framework. Subsequent reincorporation of the dissociated linker reassembles the MOF with an aperture size that is smaller than the incorporated guest.

As a proof of principle, we used the commercially available zeolitic imidazolate framework ZIF-8 as a model MOF. We also identified two criteria that would be most appropriate for a suitable guest molecule. First, to maximize guest retention, the guest molecule should be larger than the MOF aperture size. For encapsulation in ZIF-8, this requirement makes the ideal guest size between ~ 3.4 and 11.6 Å, the aperture and pore sizes of ZIF-8, respectively. Second, in order to better quantify the loading, we initially targeted guest molecules that could be easily detectable by UV–vis spectroscopy. Rhodamine 6G (R6G) was selected as an ideal candidate that meets both criteria outlined above: it is a fluorescent dye ($\lambda_{\text{max}} = 530$ nm) with a molecular diameter of 11.3 – 13.7 Å [Figure S1 in the Supporting Information (SI)]. The amounts of encapsulated R6G were determined by UV–vis spectroscopy after acid digestion of the ZIF-8 crystals.

To test whether linker exchange can facilitate guest incorporation, R6G was incubated with ZIF-8 in the presence of 2-methylimidazole (2-mim) as an exogenous linker in butanol at 100 °C for 7 days (Figure 1). Exchange of the 2-mim linker in ZIF-8 with imidazole (im) under these conditions has been reported.^{3d} After the reaction, the material, henceforth denoted as R6G@ZIF-8, took on a cloudy light-pink hue. The structure of the guest encapsulation products was characterized by transmission electron microscopy (TEM) and powder X-ray diffraction (PXRD). Both techniques showed no apparent differences after guest encapsulation, suggesting that the guest loading method was not destructive (Figures S2 and S3).

To confirm that the R6G was indeed incorporated into ZIF-8 instead of attached to its surface, a method to remove the surface-bound R6G in all samples prior to UV–vis analysis was sought. The affinity of R6G for ZIF-8 likely arises from its ester and amine functional groups, which can interact with the hydrophilic external surfaces of ZIF-8. We discovered that briefly exposing ZIF-8 to R6G at room temperature led to coloration of the MOF

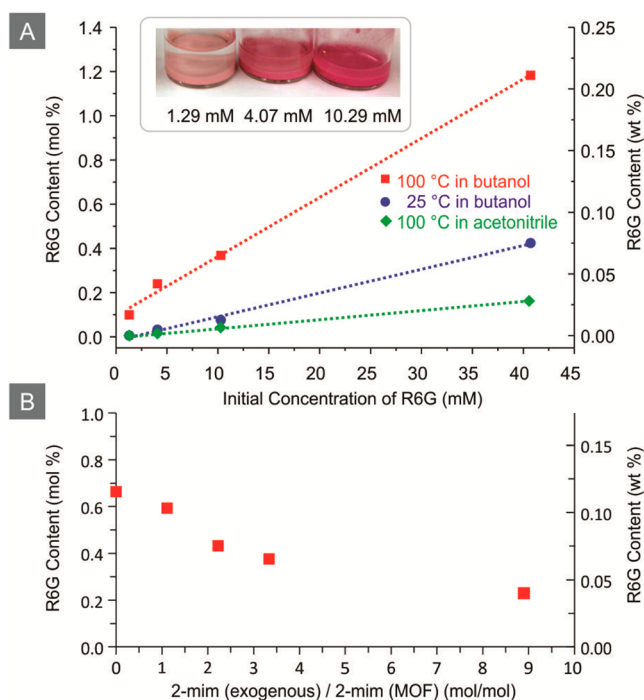


Figure 1. R6G encapsulation through ZIF-8 linker exchange. (A) R6G loading vs [R6G] at 100 °C (red) and 25 °C (blue) in *n*-butanol and at 100 °C in acetonitrile (green). The inset image shows ZIF-8 after R6G loading at various [R6G] during linker exchange at 100 °C in *n*-butanol. (B) Dependence of R6G encapsulation on [2-mim]. Conditions: 10.29 mM R6G at 100 °C in *n*-butanol for 7 days.

even though linker exchange had not occurred to an appreciable extent (Figure S4). To remove surface-bound R6G from ZIF-8, the samples were washed with methanolic solutions of polyvinylpyrrolidone (PVP), a polar polymer with polyketone functional groups that interact strongly with MOF crystals through the polyvalency effect.¹⁵ Because of its large size, PVP cannot penetrate the interior of ZIF-8. Therefore, any R6G that remains associated with ZIF-8 after PVP washing is likely trapped in the pores of ZIF-8 rather than on its surface. As expected, repeated washings of R6G@ZIF-8 with PVP led to the liberation of some R6G, but after several PVP washings, the pink color of R6G@ZIF-8 remained unchanged (Figure S5). UV–vis analysis of the PVP-washed R6G@ZIF-8 allowed the encapsulation efficiency of R6G in R6G@ZIF-8 to be quantitatively determined. A similar PVP washing procedure carried out under conditions where linker exchange does not occur led to full removal of R6G from the ZIF-8 crystals (Figure S5).

After R6G was removed from the surface, the effects of temperature, solvent, and initial concentration of R6G on R6G encapsulation in ZIF-8 were studied (Figure 1). This study indicated that the guest loading was temperature- and solvent-dependent. Higher encapsulation was observed at higher temperatures as a result of an increased linker exchange rate. Likewise, the guest loading in acetonitrile was lower because linker exchange is slower in acetonitrile than in *n*-butanol (Figure S6). As expected for diffusion-controlled guest incorporation, the R6G loading was found to be directly proportional to the initial concentration of R6G (Figure 1a). As expected for guests that are kinetically trapped, resubjection of R6G@ZIF-8 to the linker exchange reaction conditions led to diffusion of the dye into solution (Table S1 in the SI). Importantly, leaching can be

prevented by subjecting R6G@ZIF-8 to conditions where linker exchange is slow (Table S1).

To further confirm that the R6G was encapsulated in ZIF-8 during linker exchange, photophysical measurements were made (Table S2). Comparison of the normalized fluorescence intensities of R6G@ZIF-8 (prepared by linker exchange in *n*-butanol with R6G), surface-bound R6G (prepared by brief exposure of ZIF-8 to R6G), and free R6G in solution provided some insight. A dramatic decrease in fluorescence intensity was observed for R6G@ZIF-8 and surface-bound R6G compared with free R6G in solution. Moreover, the normalized intensity for surface-bound R6G (0.096) was more than double that of R6G@ZIF-8 (0.042). The lower intensity observed for R6G@ZIF-8 compared with surface-bound R6G is likely due to dye encapsulation in R6G@ZIF-8, which is expected to alter light absorption and/or emission as a result of differing interactions between the guest molecule and the framework. Regardless of the specific rationale, the difference in fluorescence intensity observed for R6G@ZIF-8 compared with surface-bound R6G provides further support that R6G is encapsulated in ZIF-8 during linker exchange instead of bound to the external ZIF-8 surface.

To gain a better understanding of the guest encapsulation process, the effect of the exogenous 2-mim linker concentration on the guest loading was explored next. Somewhat surprisingly, the R6G loading was inversely proportional to the concentration of exogenous linker (Figure 1b). In fact, the highest loading of R6G was observed when the reaction was carried out without any exogenous 2-mim linker. Although unexpected, this result could be rationalized by a dissociative linker substitution mechanism where dissociation of 2-mim from ZIF-8 led to the formation of a linker-deficient "open" state (Scheme 1). At low concentrations of free im, the "open" state is not as readily arrested by free linker, which allows more time for the guest to diffuse into the pores of the MOF. Consequently, higher guest loadings are observed at lower concentrations of exchanging linker.

To test the hypothesis that linker substitution is dissociative, we examined the kinetics of the linker exchange reaction under pseudo-first-order conditions by varying the initial concentration of exogenous im linker (for details see the SI). Observed rate constants (k_{obs}) for the linker exchange reaction were obtained using the method of initial rates (<10% conversion). PXRD indicated that the crystal structure of ZIF-8 was not perturbed under these conditions. By plotting k_{obs} versus [im], we observed a linear correlation with a nonzero slope and intercept (Figure 2). These data suggest that there is a competition between

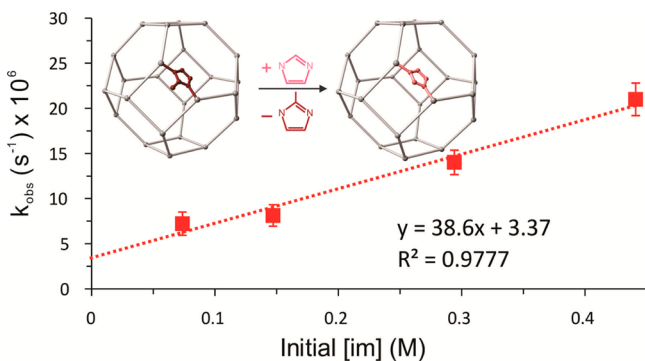


Figure 2. Observed rate constants (k_{obs}) for exchange of ZIF-8 with im at different [im].

associative and dissociative linker substitution reactions, with the slope of this line ($m = 38.6 \times 10^{-6} \text{ M}^{-1} \text{ s}^{-1}$) being the second-order rate constant for associative exchange and the intercept ($b = 3.37 \times 10^{-6} \text{ s}^{-1}$) being the first-order rate constant for dissociative exchange. Under the empirically determined conditions employed for linker exchange ($[\text{im}] = 147 \text{ mM}$), the apparent rate constant for associative linker substitution ($k_{\text{app}} = k_{\text{a}}[\text{im}]$) is $5.67 \times 10^{-6} \text{ s}^{-1}$, which is on par with the first-order rate constant for dissociative linker exchange. Importantly, under the conditions that worked best to maximize guest incorporation ($[\text{im}] = 0$), the associative exchange mechanism was completely shut down. Indeed, the lower guest incorporation seen at higher linker concentrations may be due to a competing associative exchange process that precludes the formation of an "open" state for guest incorporation. To further examine the mechanism of guest encapsulation, the relationship between the im linker exchange rate and the R6G loading was evaluated in different solvents (Figure S6). As expected, higher R6G loading was observed in solvents where the linker exchange rate is higher. Moreover, every solvent that promoted facile linker exchange also demonstrated higher guest encapsulation in the absence of exogenous 2-mim compared with reactions carried out in the presence of 2-mim.

Finally, to probe the generality of the methodology, encapsulation of a ligand suitable for incorporating transition-metal complexes in ZIF-8 was targeted. Because it is ubiquitous in organometallic catalysis and has the appropriate molecular size (Figure S1), triphenylphosphine (PPh_3) (molecular diameter = 9.56 \AA) was chosen as the initial guest ligand. The same method used for dye encapsulation was adopted to encapsulate PPh_3 in ZIF-8 (henceforth denoted as $\text{PPh}_3\text{@ZIF-8}$) using initial $[\text{PPh}_3] = 165$ and 220 mM . Elemental analysis of the product obtained with initial $[\text{PPh}_3] = 220 \text{ mM}$ indicated a PPh_3 loading of 2 wt % (Figure S7).

To demonstrate that the PPh_3 was mainly encapsulated within the pores of ZIF-8 and not on its surface, N_2 adsorption data were collected at 77 K on $\text{PPh}_3\text{@ZIF-8}$ at both loadings and commercial ZIF-8, with a high resolution of points in the micropore adsorption region (Figure 3). Saturation of the micropore volume with N_2 occurred for the reference ZIF-8 material at $485 \text{ cm}^3/\text{g}$, and the BET surface area was calculated to be $1554 \text{ m}^2/\text{g}$ using a P/P_0 range of 5×10^{-4} to 5×10^{-3} (before gating) or $1885 \text{ m}^2/\text{g}$ with a range of 5×10^{-4} to 10^{-2} (after gating). These surface areas are in agreement with ZIF-8 values from the literature.¹⁶ For the $\text{PPh}_3\text{@ZIF-8}$ samples, micropore saturation occurred at $459 \text{ cm}^3/\text{g}$ for the sample exchanged with 165 mM PPh_3 and at $405 \text{ cm}^3/\text{g}$ for that with 220 mM PPh_3 ; these values are 5% and 16% lower than for ZIF-8. This decrease in the micropore adsorption capacity was in excess of the decrease anticipated from the weight gain upon loading (only 2%) and is consistent with guests occupying some pores of the MOF. From these data, we estimated that ~ 1 in every 10 pores in ZIF-8 was occupied by a PPh_3 ligand. Such loadings are possible only by the linker exchange process that facilitates incorporation of the large ligand guest.

In summary, we have developed a method for postsynthetic encapsulation of large guests (PPh_3 , R6G) with molecular diameters that exceed the framework aperture size in ZIF-8 nanocrystals beyond what could be explained by framework flexibility. The approach capitalizes on the existence of linker exchange reactions, which were shown by our kinetic studies to proceed by a competition between associative and dissociative exchange mechanisms. Maximum guest encapsulation was

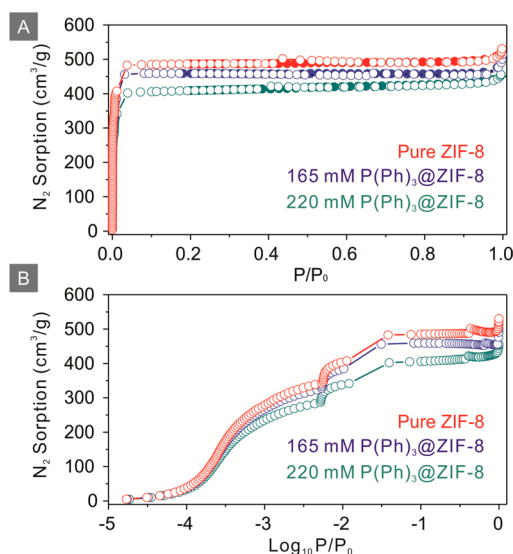


Figure 3. (A) N₂ absorption (○) and desorption (●) isotherms of ZIF-8 (red), 165 mM PPh₃@ZIF-8 (blue), and 220 mM PPh₃@ZIF-8 (green). (B) Plot vs log₁₀(P/P₀) to show the detailed N₂ sorption at low pressure.

observed under conditions where the dissociative mechanism predominates because the dissociation of at least one aperture-defining 2-mim linker facilitates the formation of a short-lived “open” state in the pore with an expanded pore aperture size. In contrast to other encapsulation strategies, this approach does not require any specific electrostatic interaction between the guest and the MOF host, which may significantly expand the scope of molecular guests and MOF hosts suitable for forming host–guest composites. In addition to the impact of these findings on the ability to incorporate large guests in MOFs, important insight into the mechanism for linker exchange processes in MOFs has been garnered. Such processes have already been exploited for the synthesis of novel MOF architectures,¹² useful catalyst species,¹⁰ and sophisticated nanocomposite materials.¹³ Future investigations will look at the application of these findings to other classes of MOFs as well as the use of the new encapsulation methodology for the development of catalysts that take advantage of the size-selective capabilities of MOFs.

■ ASSOCIATED CONTENT

Supporting Information

Procedures and additional data. This material is available free of charge via the Internet at <http://pubs.acs.org>.

■ AUTHOR INFORMATION

Corresponding Authors

jeffery.byers@bc.edu

frank.tsung@bc.edu

Author Contributions

†J.V.M. and L.-Y.C. contributed equally.

Notes

The authors declare no competing financial interest.

■ ACKNOWLEDGMENTS

This work was supported by Boston College. The authors thank Prof. D. Qu and Dr. D. Zheng at UMass-Boston for BET measurements, Prof. S. Wilson at Boston College for the use of their diffractometer, G. McMahon for assistance with TEM, and

Bryce L. Anderson in Prof. Nocera’s group at Harvard University for picosecond time-resolved fluorescence spectroscopy.

■ REFERENCES

- (1) (a) Horcajada, P.; Chalati, T.; Serre, C.; Gillet, B.; Sebrie, C.; Baati, T.; Eubank, J. F.; Heurtaux, D.; Clayette, P.; Kreuz, C.; Chang, J.-S.; Hwang, Y. K.; Marsaud, V.; Bories, P.-N.; Cynober, L.; Gil, S.; Férey, G.; Couvreur, P.; Gref, R. *Nat. Mater.* **2010**, *9*, 172. (b) Rimoli, M. G.; Rabaioli, M. R.; Melisi, D.; Curcio, A.; Mondello, S.; Mirabelli, R.; Abignente, E. *J. Biomed. Mater. Res.* **2008**, *87A*, 156. (c) Yanai, N.; Kitayama, K.; Hijikata, Y.; Sato, H.; Matsuda, R.; Kubota, Y.; Takata, M.; Mizuno, M.; Uemura, T.; Kitagawa, S. *Nat. Mater.* **2011**, *10*, 787. (d) McGilvray, K. L.; Chretien, M. N.; Lukeman, M.; Scaiano, J. C. *Chem. Commun.* **2006**, 4401. (e) Talin, A. A.; Centrone, A.; Ford, A. C.; Foster, M. E.; Stavila, V.; Haney, P.; Kinney, R. A.; Szalai, V.; El Gabaly, F.; Yoon, H. P.; Leonard, F.; Allendorf, M. D. *Science* **2014**, *343*, 66. (f) Cardin, D. J. *Adv. Mater.* **2002**, *14*, S53. (g) Muller, M.; Devaux, A.; Yang, C. H.; De Cola, L.; Fischer, R. A. *Photochem. Photobiol. Sci.* **2010**, *9*, 846. (h) Calzaferri, G.; Huber, S.; Maas, H.; Minkowski, C. *Angew. Chem., Int. Ed.* **2003**, *42*, 3732. (i) Martínez-Martínez, V.; Furukawa, S.; Takashima, Y.; López Arbeloa, I.; Kitagawa, S. *J. Phys. Chem. C* **2012**, *116*, 26084. (j) Wang, J. L.; Wang, C.; Lin, W. B. *ACS Catal.* **2012**, *2*, 2630. (k) Son, H. J.; Jin, S. Y.; Patwardhan, S.; Wezenberg, S. J.; Jeong, N. C.; So, M.; Wilmer, C. E.; Sarjeant, A. A.; Schatz, G. C.; Snurr, R. Q.; Farha, O. K.; Wiederrecht, G. P.; Hupp, J. T. *J. Am. Chem. Soc.* **2013**, *135*, 862. (l) Dutta, P. K.; Severance, M. *J. Phys. Chem. Lett.* **2011**, *2*, 467.
- (2) Corma, A.; Garcia, H. *Eur. J. Inorg. Chem.* **2004**, 1143.
- (3) (a) Fletcher, A. J.; Thomas, K. M.; Rosseinsky, M. J. *J. Solid State Chem.* **2005**, *178*, 2491. (b) Costa, J. S.; Gamez, P.; Black, C. A.; Roubeau, O.; Teat, S. J.; Reedijk, J. *Eur. J. Inorg. Chem.* **2008**, 1551. (c) Kim, M.; Cahill, J. F.; Fei, H.; Prather, K. A.; Cohen, S. M. *J. Am. Chem. Soc.* **2012**, *134*, 18082. (d) Karagiari, O.; Lalonde, M. B.; Bury, W.; Sarjeant, A. A.; Farha, O. K.; Hupp, J. T. *J. Am. Chem. Soc.* **2012**, *134*, 18790.
- (4) (a) Li, B.; Zhang, Y.; Ma, D.; Ma, T.; Shi, Z.; Ma, S. *J. Am. Chem. Soc.* **2014**, *136*, 1202. (b) Alkordi, M. H.; Liu, Y.; Larsen, R. W.; Eubank, J. F.; Eddaoudi, M. *J. Am. Chem. Soc.* **2008**, *130*, 12639. (c) Larsen, R. W.; Wojtas, L. *J. Mater. Chem. A* **2013**, *1*, 14133.
- (5) Lee, J.; Farha, O. K.; Roberts, J.; Scheidt, K. A.; Nguyen, S. T.; Hupp, J. T. *Chem. Soc. Rev.* **2009**, *38*, 1450.
- (6) Zhuang, J.; Kuo, C.-H.; Chou, L.-Y.; Liu, D.-Y.; Weerapana, E.; Tsung, C.-K. *ACS Nano* **2014**, *8*, 2812.
- (7) Fei, H.; Cahill, J. F.; Prather, K. A.; Cohen, S. M. *Inorg. Chem.* **2013**, *52*, 4011.
- (8) Karagiari, O.; Bury, W.; Sarjeant, A. A.; Stern, C. L.; Farha, O. K.; Hupp, J. T. *Chem. Sci.* **2012**, *3*, 3256.
- (9) Kim, M.; Cahill, J. F.; Su, Y.; Prather, K. A.; Cohen, S. M. *Chem. Sci.* **2012**, *3*, 126.
- (10) Pullen, S.; Fei, H.; Orthaber, A.; Cohen, S. M.; Ott, S. *J. Am. Chem. Soc.* **2013**, *135*, 16997.
- (11) Deria, P.; Mondloch, J. E.; Tylianakis, E.; Ghosh, P.; Bury, W.; Snurr, R. Q.; Hupp, J. T.; Farha, O. K. *J. Am. Chem. Soc.* **2013**, *135*, 16801.
- (12) Burnett, B. J.; Barron, P. M.; Hu, C.; Choe, W. *J. Am. Chem. Soc.* **2011**, *133*, 9984.
- (13) Takaishi, S.; DeMarco, E. J.; Pellin, M. J.; Farha, O. K.; Hupp, J. T. *Chem. Sci.* **2013**, *4*, 1509.
- (14) Bury, W.; Fairen-Jimenez, D.; Lalonde, M. B.; Snurr, R. Q.; Farha, O. K.; Hupp, J. T. *Chem. Mater.* **2013**, *25*, 739.
- (15) Lu, G.; Li, S.; Guo, Z.; Farha, O. K.; Hauser, B. G.; Qi, X.; Wang, Y.; Wang, X.; Han, S.; Liu, X.; DuChene, J. S.; Zhang, H.; Zhang, Q.; Chen, X.; Ma, J.; Loo, S. C. J.; Wei, W. D.; Yang, Y.; Hupp, J. T.; Huo, F. *Nat. Chem.* **2012**, *4*, 310.
- (16) Park, K. S.; Ni, Z.; Cote, A. P.; Choi, J. Y.; Huang, R. D.; Uribe-Romo, F. J.; Chae, H. K.; O’Keeffe, M.; Yaghi, O. M. *Proc. Natl. Acad. Sci. U.S.A.* **2006**, *103*, 10186.